Structural and magnetic properties of a nanocrystalline $Fe_{75}Nb_{10}Si_5B_{10}$ alloy produced by mechanical alloying

J.J. Suñol[1*], L. Escoda[1], J. Fort[1], J. Pérez[1], T. Pujol[1].

[1] *EPS (P II). Universitat de Girona, Campus Montilivi s/n, 17071 Girona, Spain.*

*Corresponding author: Tel: +34-972-418490; fax: +34-972-418098.

E-mail adress: joanjosep.sunyol@udg.es

Keywords: Mechanical alloying; soft magnetic properties; nanomaterials.

Abstract

In this paper we present the structural and magnetic analysis of a nanocrystalline $Fe_{75}Nb_{10}Si_5B_{10}$ alloy produced by mechanical alloying. The effects of milling time on microstructure, thermal behavior and magnetic properties were studied by X-ray diffraction (XRD), differential scanning calorimetry (DSC) and vibrating sample magnetometry (VSM). By controlling the milling and annealing conditions an improvement in the magnetic properties was found.

1. Introduction

Mechanical alloying (MA) is a process able to prepare powdered alloys. Solid state reactions occur when materials are processed in a ball mill. Nanostructured Fe-based soft magnetic materials as a new class of engineering materials (whit enhanced properties and crystalline size between 1 and 100 nm) can be produced by mechanical driven forces by MA [1,2]. These materials have advantages in applications like: electric and magnetic measurements, transformer magnets, information storage and magnetic cores [3].

One of the main problems of the MA powders is that usually exhibits low soft magnetic properties that the melt-spun ribbons of the same composition [4,5]. Furthermore, the thermal stability of the amorphous and/or nanocrystalline phase is also lower in the MA alloys [6]. Nevertheless, appropriate milling conditions can minimize this effect. Final alloy properties were influenced by milling conditions, i.e. the use of a process control agent (PCA). A PCA is a surface additive normally used in the milling processes in order to control the balance between the fracture and welding. The mechanism lies in the modification on the surface condition of the deformed particles by impeding the clean powder to powder contact necessary for cold welding [7]. The type and amount of PCA also plays an important role in the balance. Likewise, it is possible to modify the final microstructure as well as the functional properties of materials. A crystallite size reduction and high thermal stability can be found [8,9], minimizing differences with as quenched alloys.

In this work we have investigated the evolution of the alloy structure during the milling process and the magnetic properties of the $Fe_{75}Nb_{10}Si_5B_{10}$ alloy. It is the first time that this alloy has been developed by mechanical alloying. The Fe-Nb-B system it has been shown that exhibits the smallest grain size in the Cu free Fe-M-B alloys

(where M = Zr, Nb, Hf) [10]. Moreover, the introduction of Si favors higher electrical resistivity in Fe-Si alloys in comparison with pure Fe powder [11].

2. Experimental

Mechanical alloying was carried out in a planetary high-energy ball mill (Fritsch Pulverisette P7) starting from pure elements: Fe (99.7% purity and particle size under 8μm); Nb (99.85% purity and particle size under 74μm); Si (99.9 % purity and particle size under 45μm) and B (99.6% purity and particle size 50μm). Mechanical milling was carried out at 700 rpm under Ar atmosphere, using hardened steel balls and vials. The ball to powder weight ratio was 5:1. The milling times were: 5h, 20h, 40h, 100h and 200h. Cyclohexane was used as PCA.

Thermal stability of milled samples milled was analyzed by differential scanning calorimetry (DSC). The grain size reduction and the formation of nanocrystalline structure and soft magnetic properties of mechanically alloyed $Fe_{75}Nb_{10}Si_5B_{10}$ were evaluated by X-ray diffraction (XRD) using CuKα radiation, scanning electron microscopy (SEM) operating at 15 KV and vibrating sample magnetometry (VSM) with applied field of 1 T. Contamination was followed by energy dispersive X-ray spectroscopy (EDX) using a Si-Li detector, by induction coupled plasma (ICP) and by chemical analysis to determine the C content.

3. Results and discussion

Thermal study was performed by differential scanning calorimetry. Stability, an important factor on metastable structures is here related to the relaxation phenomena

and crystallization. Figure 1 show DSC curves corresponding to alloys milled from 5 to 200h. All DSC scans show several exothermic reactions on heating. At low temperature, beginning at about 430 K, a broad hump for milling times higher than 5h. This is a signature of stress recovery, that is, deformation energy stored during the milling process. Since it occurs in a wide temperature range it is often overlapped at high temperatures with exothermic peaks characteristic of crystallization processes. In a previous work in the Fe-Nb-B system, the broad exothermic peaks were related to the crystalline growth of different environments of the bcc Fe rich phase [12]. In our study, after 200h of milling only one main crystallization peaks remains indicating a more homogeneous alloy than samples milled at lower times. The reported second crystallization stage (>900 K) associated to the formation of intermetallic phases [13] in Fe-Nb-B alloys was not here analyzed.

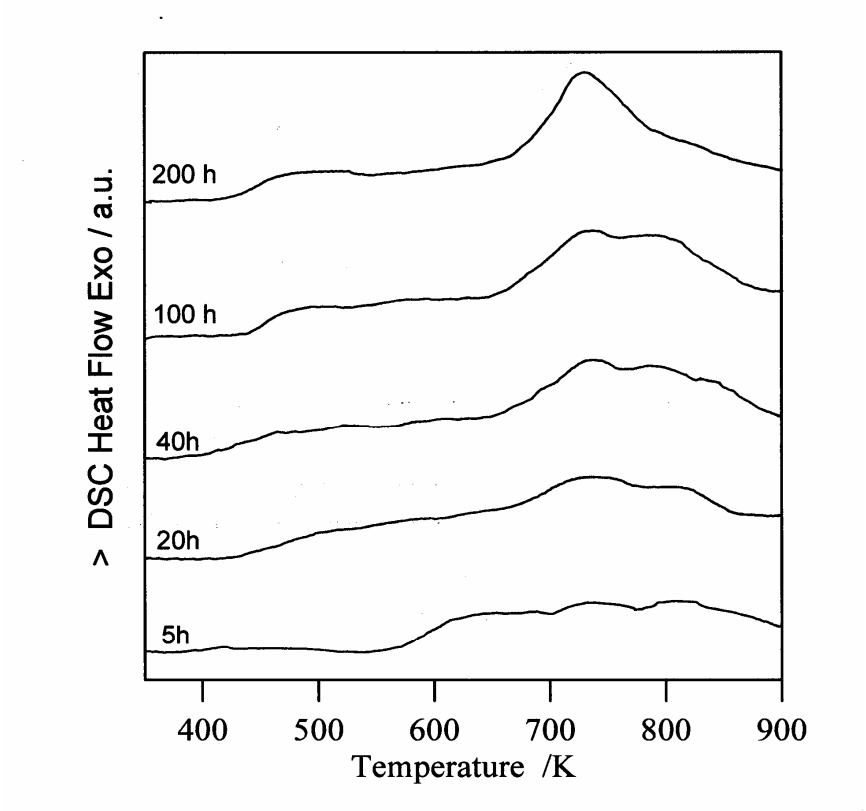

Figure 1

The apparent activation energy, *E*, for the main crystallization process of alloys milled 200h was evaluated using the Kissinger equation: $\ln(\beta/T_p^2)$ versus $1/T_p$ with β the heating rate and T_p the peak temperature [14] of the assumed peak position selected as the maximum value of the DSC curve. The crystallization data were obtained from DSC scans at different heating rates: 2.5, 5, 10, 20 and 40 K min^{-1}. The activation energy, 302 ± 28 kJ mol^{-1}, is associated with a grain growth process. From the literature, the grain growth activation energy of pure Fe is 174 kJ mol^{-1} for grain boundary diffusion and 251-282 kJ mol^{-1} for lattice diffusion [15] but the introduction of other elements may increase/decrease this value. Energies of 238 and 290 kJ mol^{-1} have be found in other Fe-B based nanocrystalline alloys [16,17].

DSC analysis was confirmed with complementary structural study performed by X-ray diffraction. From the XRD diffraction patterns (see figure 2) the average grain size and the internal microstrain were estimated by Williamson-Hall method [18] taking into account the instrumental broadening for the calculations. Figure 3 shows the values of crystalline size, microstrain and lattice parameter as a function of milling time. As usual in MA powders, when increasing the milling time until 100h the crystallite size decreases and the internal microstrain increases. Furthermore, the lattice parameter decreases at low milling time and increases at high milling time indicating the presence of other elements in solid solution into the bcc Fe rich phase. The lattice contraction is in good agreement with dissolution of Si atoms into bcc Fe structure [19] and lattice expansion is in good agreement with B dissolution [12]. After 100h of milling only minor change was found. The reduction of internal stress is associated to a more homogeneous alloy.

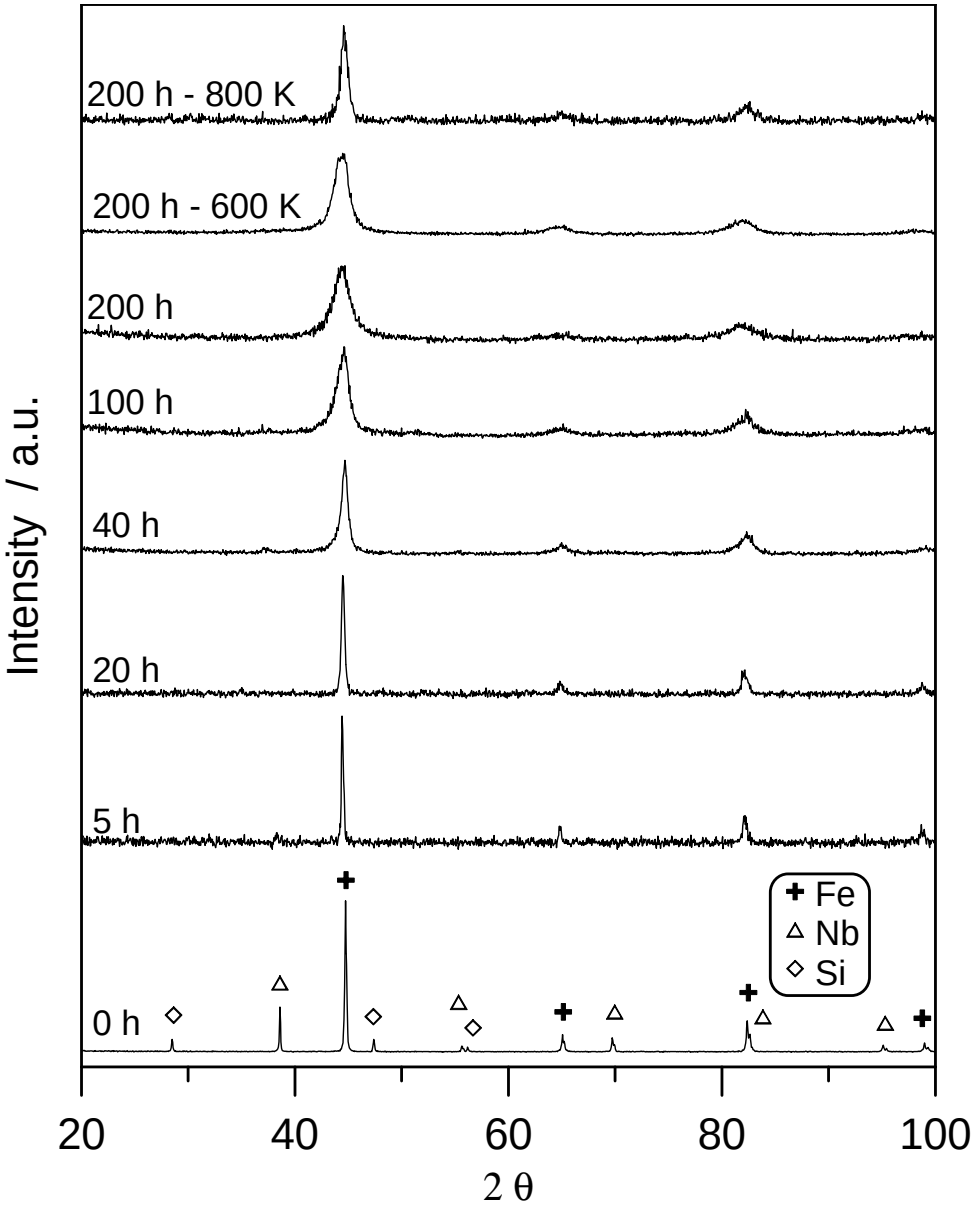

Figure 2

Alloy milled for 200h was annealed at two temperatures: 600 K and 800 K. XRD parameters are also given in figure 3. Thermal treatments induce the reduction of the internal microstrain and the nanocrystalls growth. After annealing at 600K the microstrain diminishes whereas the crystallite size remains stable. The relatively low crystallite size increase, from 9 to 23 nm after annealing at 800K, confirms the high thermal stability of the nanocrystalline phase. Similar behavior was found in a Fe-Zr based alloy milled with cyclohexane as PCA [9].

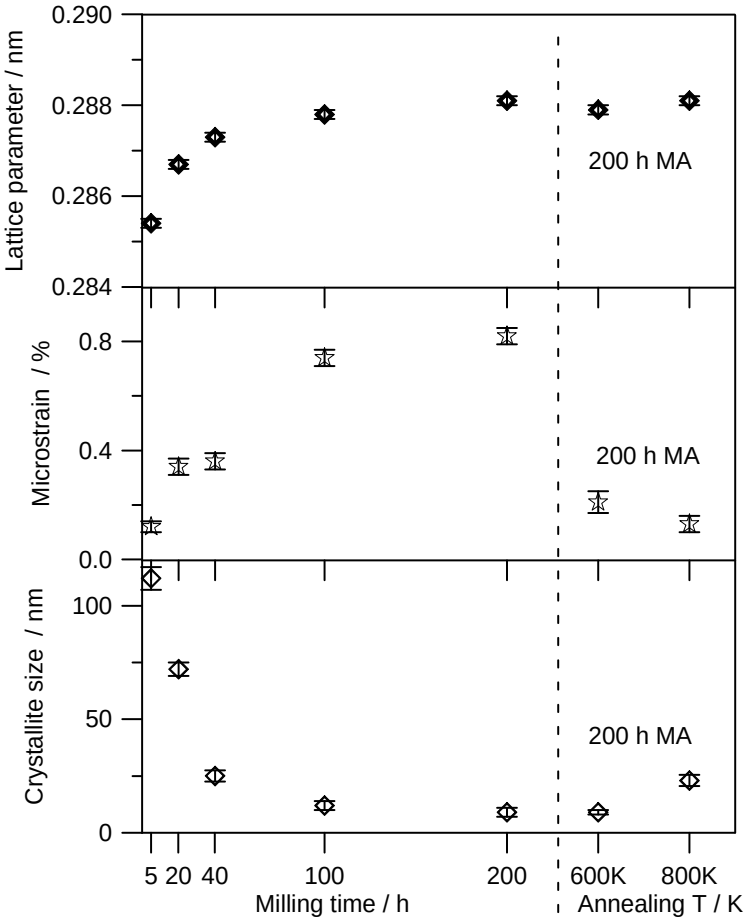

Figure 3

The magnetic properties of as milled $Fe_{75}Nb_{10}Si_5B_{10}$ alloy, i.e. coercivity H_c and saturation magnetization M_s for different milling times and annealing temperatures are given in figure 4.

Saturation magnetization increases, from 138 to 168 emu/g, after 5 and 200 hours of milling respectively. Annealing also provokes an increase of saturation magnetization to 182 emu/g. Coercivity increase with milling time from 73 to 125 Oe and diminishes after annealing at 600K to 57 Oe. The saturation magnetization values are comparable to Fe-Nb-B alloys developed by melt-spinning whereas coercivity is higher [20,21].

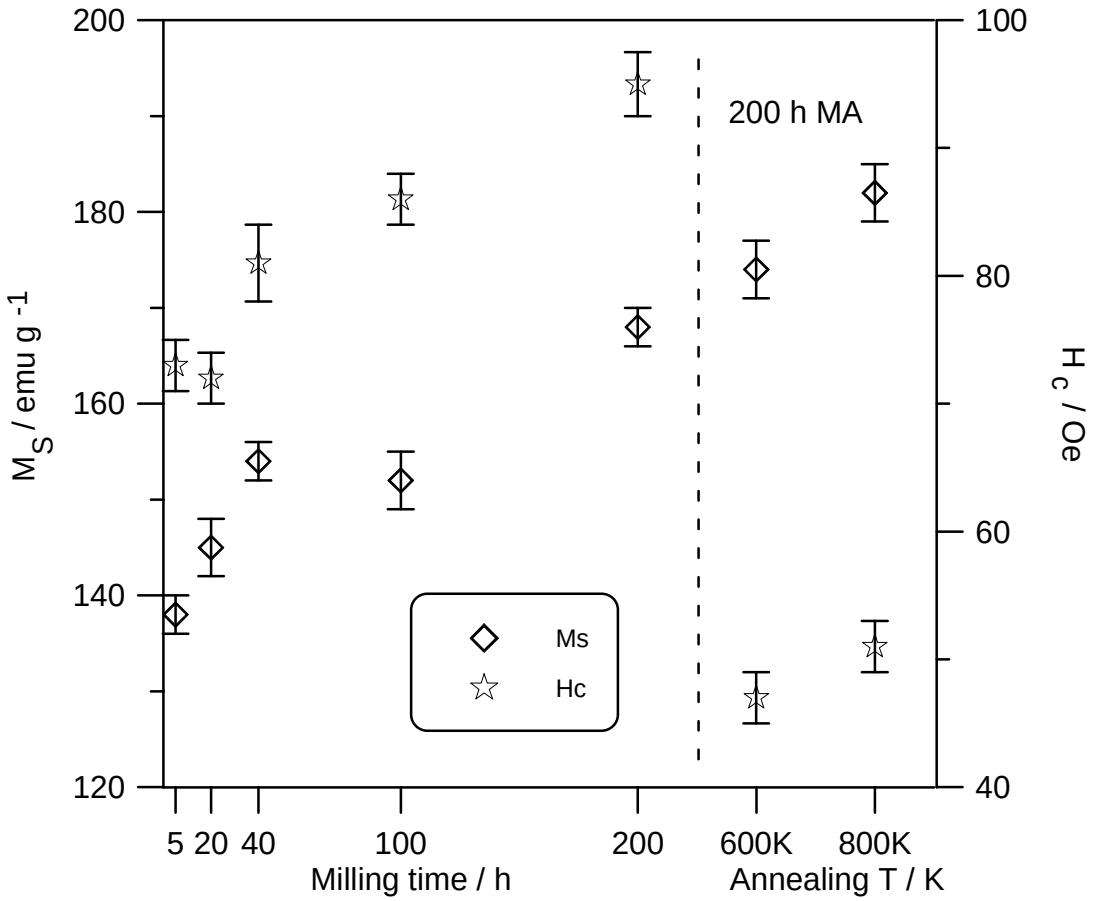

Figure 4

It is worth nothing that the soft magnetic properties, low coercivity and high saturation magnetization, can be improved by minimizing the magnetic domain wall movement and minimizing the domain wall rotation [22]. The magnetic properties are influenced by internal microstrain that inhibits the magnetic domain wall rotation. Furthermore, the improvement of soft magnetic properties during annealing may be explained by the decrease in the volume fraction of the residual intergranular highly disordered phase [20]. For it, the diminution/augmentation of coercivity/saturation magnetization by annealing is associated to microstructure changes. In order to improve the magnetic properties of this type of alloys further investigations are needed concerning the optimization of the milling and annealing regimes.

Contamination was analyzed in sample milled for 200h. The EDX and ICP analysis shows a slight increase of Fe content (< 1.5 at.%) as well as Cr (<0.4 at%) due to milling

tools. The C content as determined by chemical analysis is lower than 0.2 at%. This minor contamination prevents the formation of carbide formation as detected in Fe-Nb-B milled alloys [21,22].

Conclusions

We have succeeded in the development by mechanical alloying of a nanocrystalline $Fe_{75}Nb_{10}Si_5B_{10}$ soft magnetic material. During milling, saturation magnetization and coercivity increases to 168 emu/g and 125 Oe respectively. Annealing provokes an increase of saturation magnetization to 182 emu/g. The coercivity diminishes after annealing at 600K to 57 Oe. The good magnetic properties are influenced by microstructure, i.e. low microstrain and crystallite size. Minor contamination from milling tools or process control agent was detected.

Acknowledgments

Financial support from MICYT MAT2006-13925-C02-02 (FEDER) and DURSI 2005SGR-00201 projects is acknowledged.

References

[1] J. Fecht, Scr. Mater. 44 (2001) 1719-1723.

[2] A. Bahrami, H.R. Madaah Hosseini, P. Abachi and S. Miraghaei, Mater. Letters 60 (2006) 1068.-1070.

[3] M.E. McHenry, M.A. Willard and D.E. Laughlin, Prog. In Mater. Sci., 44 (1999) 291.

[4] W. Guo, F. Padella, M. Magini and C. Colella, Mater. Sci. Forum 235 (1997) 395.

[5] C. Stiller, E. Wu, S.J. Campbell, A. Kerr, W.A. Kaczmarek, J.S. williams, J. Eckert and L. Schulz, Mater. Sci. Forum, 269 (1998) 425. [4] L. Liu, Y.F. Zhang. J. Alloys Compd. 290 (1999) 279-283.

[6] J.J. Suñol, A. González, J. Saurina, L. Escoda, L. Fernández-Barquín, J. Non-Cryst. Solids, 353 (2007) 865-868.

[7] L. Liu, Y.F. Zhang, J. Alloys Compd. 290 (1999) 279-283.

[8] M. Pilar, J.J. Suñol, J. Bonastre and L. Escoda, J. Non-Cryst. Solids 35 (2007) 848-850.

[9] R. Juárez, J.J. Suñol, R. Berlanga, J. Bonastre, L. Escoda, J. Alloys Comp., 434-435 (2007) 472-476.

[10] I. Skorvanek, J. Kovacs, J. Marcin, P. Duhaj, R. Gerling, J. Mag. Magn. Mater., 203 (1999) 226-228.

[11] A. Gupta, P. Dhuri, J. Mater. Sci. Eng. A304-306 (2001) 394-398.

[12] J.J. Suñol, A. González, J. Saurina, L. Escoda and P. Bruna, Mater. Sci. Eng. A 375-377 (2004) 874-880.

[13] J. Torrents-Serra, J. Rodríguez-Viejo, M.T. Clavaguera-Mora, J. Non-Cryst. Sol., 353 (2007) 842-844.

[14] H. Kissinger, Anal. Chem. 29 (1957) 1702.

[15] T.R. Malow and C.C. Koch, Acta. Mater., 45 (1997) 2177.

[16] J.J. Suñol, A. González, J. Saurina, J. Therm. Anal. Calorim., 72 (2003) 329-333.

[17] J. Bonastre, L. Escoda, A. González, J. Saurina and J.J. Suñol, J. Therm. Anal. Calori., 88 (2007) 83-86.

[18] G.K. Williamson and W.H. Hall, Acta Met. 1 (1953) 22-31.

[19] H.R. Madaah Hosseini and A. Bahrami, Mater. Sci. Eng. B 123 (2005) 74-79.

[20] A. Makino, T. Hatanai, A. Inoue and T. Masumoto, Mater. Sci. Eng. A226-228 (1997) 594-602.

[21] Z. Caamaño, G. Pérez, L.E. Zamora, S. Suriñach, J.S. Muñoz and M.D. Baró, J. Non-Cryst. Solids 287 (2001) 15-19.

[22] Y.I. Yang, J. Kim and D.H. Shin, J. Mater. Sci. Eng. B 78 (2000) 113-118.

Figure captions

Figure 1: DSC scans of the $Fe_{75}Nb_{10}Si_5B_{10}$ alloy at different milling times. Heating rate: 10 K/min.

Figure 2: X-ray diffraction patterns of $Fe_{75}Nb_{10}Si_5B_{10}$ alloy at different milling times. Annealing was performed in alloy milled 200 h.

Figure 3: X-ray diffraction parameters: crystallite size, internal microstrain and lattice parameter as a function of milling time and annealing temperature. Annealing was performed in alloy milled 200 h.

Figure 4: Saturation magnetization and coercivity as a function of milling time and annealing temperature. Annealing was performed in alloy milled 200 h.